Nadir Echo Removal in Synthetic Aperture Radar via Waveform Diversity and Dual-Focus Postprocessing

Michelangelo Villano, *Member, IEEE*, Gerhard Krieger, *Fellow, IEEE*, and Alberto Moreira, *Fellow, IEEE*

***Abstract*— Synthetic aperture radar (SAR) remote sensing allows high-resolution imaging independent of weather conditions and sunlight illumination and is, therefore, very attractive for the systematic observation of dynamic processes on the earth's surface. However, as a consequence of the pulsed operation and side-looking geometry of SAR, nadir echoes may significantly affect the SAR image quality, if the pulse repetition frequency is not conveniently constrained in the design of the SAR system. As the nadir interference constraint typically limits both the swath width and the ambiguity performance of the SAR system, the investigation of novel concepts for nadir echo removal is of great interest. This letter describes how to design an SAR system without the nadir interference constraint and how to remove (not only smear) the nadir echoes by means of waveform diversity on transmit and appropriate postprocessing. The proposed technique yields improved image quality and can be exploited in a similar manner for range ambiguity suppression with remarkable benefits for the design of novel SAR systems.**

***Index Terms*— Cyclically shifted chirps, matched filtering, nadir echo, pulse repetition frequency (PRF), range ambiguities, synthetic aperture radar (SAR), waveform diversity.**

I. Introduction

SYNTHETIC aperture radar (SAR) is a remote sensing technique, capable of providing high-resolution images independent of weather conditions and sunlight illumination. This makes SAR very attractive for the systematic observation of dynamic processes on the earth's surface. Typical SAR systems carry a side-looking radar antenna and transmit pulses of electromagnetic radiation downward to the surface to be imaged (i.e., the swath) at a given pulse repetition frequency (PRF). The radiated pulses spread out, interact with the surface, and propagate back to the radar, which samples the returning echoes coherently, i.e., it retains both amplitude and phase, and stores the data for future processing [1].

An inherent consequence of the pulsed operation of SAR is that the echoes of periodically transmitted pulses, propagating back from the nadir, i.e., the point with the closest distance to the radar, come back at the radar simultaneously with the echoes of interest. In particular, denoting as h the height of the platform, which carries the radar antenna, the echo from a scatterer at nadir is superimposed on the echo from a scatterer in the scene at slant range R_0, if the following condition holds:

$$R_0 = h + k\frac{c_0}{2\mathrm{PRF}} \tag{1}$$

where k is an integer number and c_0 is the speed of light in free space [2].

Although the radar antenna is designed to limit the energy transmitted to and received from the nadir direction, due to the smaller range and the specific characteristics of the scattering process (specular reflection), the nadir echo may be even stronger than the desired one and may, therefore, significantly affect the quality of the SAR image. In particular, the nadir echo appears as a bright stripe in the image (Fig. 1) [3].

The nadir interference is usually avoided by constraining the PRF selection in the design of the SAR system. Fig. 2 shows the timing diagram of an SAR, in which for a given PRF, the blue zones represent ground ranges that cannot be imaged due to the transmit interference, i.e., because the radar cannot receive while it is transmitting, while the green zones represent ground ranges that cannot be imaged due to the nadir interference, i.e., the presence of the nadir echo in the imaged scene. The imaged swaths are selected by choosing PRFs for

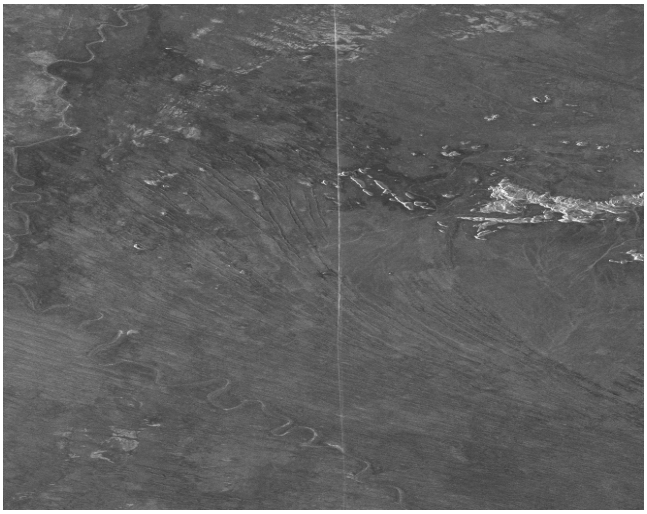

Fig. 1. Example of nadir echo in an SAR image, acquired by the TerraSAR-X satellite over Australia. The nadir echo appears as a bright vertical stripe in the middle of the image. The horizontal and vertical axes represent slant range and azimuth, respectively.

Manuscript received October 25, 2017; revised January 8, 2018; accepted February 16, 2018. *(Corresponding author: Michelangelo Villano.)*

The authors are with the German Aerospace Center (DLR), Microwaves and Radar Institute, 82234 Wessling, Germany (e-mail: michelangelo.villano@dlr.de).

Color versions of one or more of the figures in this letter are available online at http://ieeexplore.ieee.org.

Digital Object Identifier 10.1109/LGRS.2018.2808196

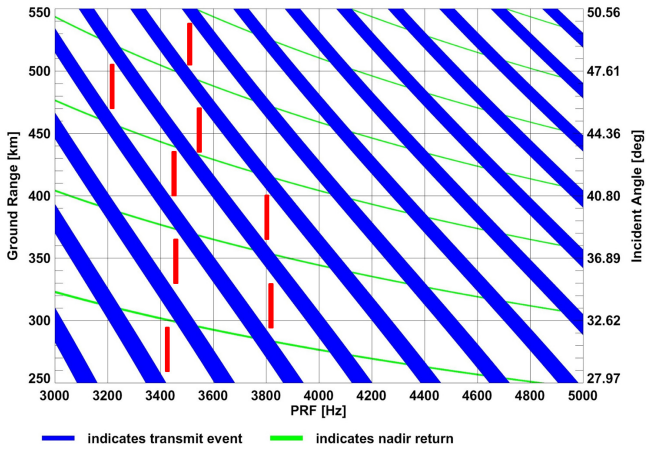

Fig. 2. Timing diagram for an SAR. The blue and green zones represent transmit and nadir interferences, respectively. The red stripes indicate some of the swaths, which can be selected.

which neither transmit nor nadir interferences occur (see red stripes in Fig. 2) [2].

However, the additional constraint on the PRF selection imposed by the nadir interference typically limits both the swath width and the ambiguity performance of SAR systems. In order to meet given requirements in terms of ambiguity performance, it might, therefore, be necessary to increase the system complexity by, e.g., increasing the size of the radar antenna.

This letter presents an innovative concept for nadir echo suppression, which exploits the waveform diversity on transmit and the use of different matched filters in the processing for the removal of the nadir echo [4]. The rationale of the technique is described in Section II, while an example of implementation with an assessment of the nadir echo suppression performance is shown in Section III. Conclusions are drawn in Section IV, where the impact of waveform alternation on image quality and, as a possible extension, the applicability of the technique to range ambiguity suppression are discussed.

II. Rationale

The echo of a subsequently transmitted pulse, propagating back from the nadir and coming back at the radar simultaneously with the echo of interest, can be smeared as a result of the pulse or range-compression operation, if different "orthogonal" waveforms are used for the two transmitted pulses. This was already proposed for the suppression of range ambiguities in [5]–[7], where up and down chirps are alternated. If k in (1) is odd, e.g., $k = 3$, nadir echoes and all odd near and far range ambiguities will be smeared. Up and down chirps are only examples of orthogonal waveforms, for which a comprehensive discussion can be found in [8]. The smeared nadir echoes, resulting for mere waveform alternation, however, although less visible, still contribute to the background noise, decrease the image contrast, and may limit the retrieval of information from SAR data.

While keeping the waveform diversity concept, the proposed technique allows removing (not only smearing) the nadir echo through a dedicated dual-focus postprocessing technique,

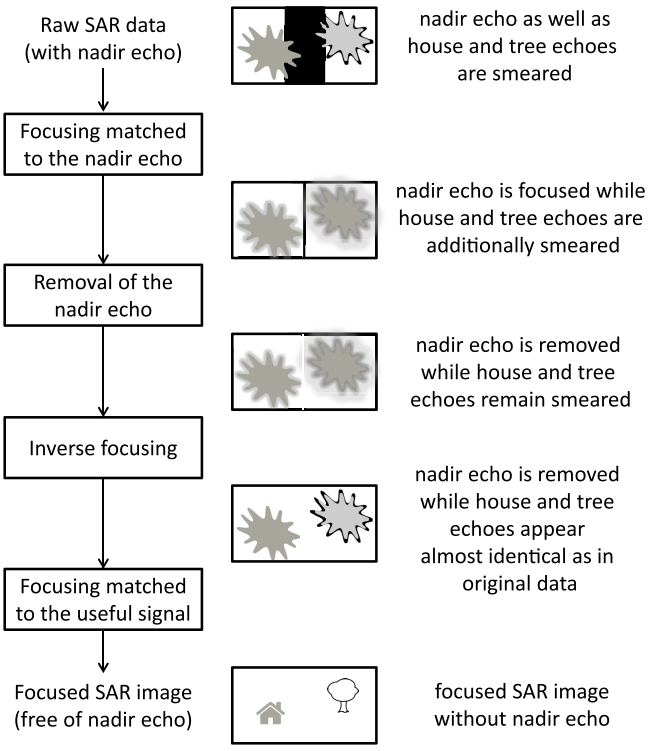

Fig. 3. Block diagram highlighting the processing steps required to suppress the nadir echo in an SAR system with waveform diversity. The useful signal is schematically represented by a house and a tree, in the left and right parts of the image, respectively, while the nadir interference is located in the middle of the image.

which exploits the nadir echo's sparsity in range-compressed SAR data. In particular, the acquired raw data are focused using a filter "matched" to the nadir echo, so that the nadir echo can be removed with a negligible corruption of the useful signal, as the nadir echo is focused and located at specific ranges, while the useful signal is smeared. Through an inverse focusing operation, the latter focused data, in which the nadir echo has been removed, are then transformed back into raw data and finally focused using a filter that is "matched" to the useful signal. If the sequence of employed waveforms is properly selected, a focused SAR image is obtained, in which the nadir echo is significantly attenuated, while the useful signal is only minimally affected. The block diagram in Fig. 3 highlights the processing steps required to suppress the nadir echo in an SAR system, in which different waveforms are alternated on transmit. The useful signal is schematically represented by a house and a tree, in the left and right parts of the image, respectively, while the nadir interference is located in the middle of the image.

Once raw data are focused with a filter matched to the nadir echo, the nadir echo can be simply removed by blanking the pixels, where it is located. In particular, the location of the nadir echo can be determined from the PRF, the orbit information, and a digital elevation model of the area of interest. It is also possible to apply an adaptive threshold to the image obtained after focusing matched to the nadir echo, performing the nadir echo suppression only if the image is indeed corrupted. In an SAR system with waveform diversity,

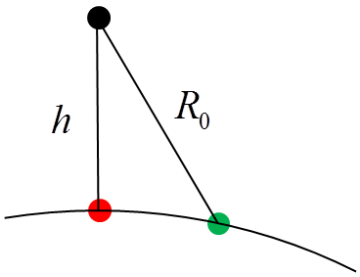

Fig. 4. Simplified scenario with only two point-like targets, located in the scene (green) and at nadir (red), respectively.

in fact, the nadir echo is smeared in the SAR image obtained after focusing matched to the useful signal and, in some cases, the level of the smeared nadir echo signal can be much lower than that of the thermal noise.

The proposed technique should not be confused with azimuth phase coding, i.e., the application of an azimuth phase modulation to the transmitted pulses and a corresponding phase demodulation to the received pulses, which is effective for range ambiguity and nadir echo suppression, as long as the PRF exceeds the processed Doppler bandwidth [9].

III. Design Example

In the following, an example of implementation of the proposed technique is presented together with an assessment of the nadir echo suppression capabilities. For the purpose of illustration, a simple scenario is considered, in which only two point-like targets,[1] located in the scene and at the nadir, respectively, are present (Fig. 4), and k in (1) is equal to 1.

The following waveforms (cyclically shifted chirps, an example of short-term shift-orthogonal waveforms [10], proposed in [6]) are employed on transmit:

$$s_i(t) = \begin{cases} e^{j\pi \frac{B}{T}\left(t - t_i - T\left(\left\lfloor \frac{t+\frac{T}{2}-t_i}{T} \right\rfloor\right)\right)^2}, & -\frac{T}{2} \le t \le \frac{T}{2} \\ 0, & \text{otherwise} \end{cases} \quad (2)$$

where T is the waveform (or chirp) width, B is the waveform (or chirp) bandwidth, and t_i, $-T/2 \le t_i < T/2$, is the cyclical shift of the chirp waveform. Fig. 5 schematically shows the radio frequency signals and the time–frequency diagrams of a conventional (nonshifted) chirp and a cyclically shifted chirp.

In particular, a sequence of waveforms is employed, which repeats then periodically, where T and B remain constant for all waveforms and t_i is varied from pulse to pulse according to the following quadratic law:

$$t_i = \frac{i(i+1)}{2B} - T\left\lfloor \frac{i(i+1)+BT}{2BT} \right\rfloor, \quad i = 0..2BT-1. \quad (3)$$

Furthermore, the received echoes are not processed using the usual matched filter, but the ideal filter proposed in [11].

[1]Due to specular reflection the Doppler spectrum of the nadir echo could be narrower than that of the useful signal and determine a widening of the impulse response of the nadir echo in the azimuth direction, which would nevertheless not influence the removal of the nadir echo.

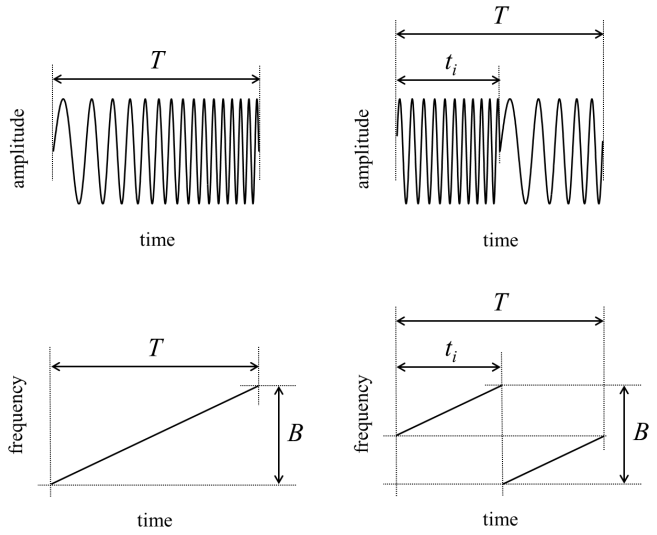

Fig. 5. Schematic representation of the (Top) radio frequency signals and the (Bottom) time–frequency diagrams of a conventional, (Left) nonshifted chirp, and (Right) cyclically shifted chirp.

TABLE I
System and Processing Parameters

Parameter	Value
Wavelength	0.229 m (L-band)
Orbit height	628 km
Antenna length	9.9 m
Chirp bandwidth	38 MHz
Chirp duration	132.89474 μs
PRF	2000 Hz
Processed Doppler bandwidth	1670 Hz
Processing window in range	Generalized Hamming, α = 0.6
Processing window in azimuth	Generalized Hamming, α = 0.6

Using the system and processing parameters provided in Table I, the nadir echo suppression results of a simulation are presented, assuming that the useful signal and the nadir echo are superimposed in the raw data and have equal energy.

Fig. 6 shows the raw, range-compressed, and focused data, in case the sequence of waveforms of (2) and (3) is employed, but the raw data are simply focused using a filter "matched" to the useful signal. The nadir echo appears smeared in the focused data, but it still contributes to the background noise.

Fig. 7 refers instead to the case in which the sequence of waveforms of (2) and (3) is employed and data are processed according to the described technique. Raw data are first focused using a filter "matched" to the nadir signal. Using the cyclically shifted chirps, the useful signal after range-compression signal is dislocated at different ranges [see Fig. 7(b)][2] and then smeared over azimuth as a consequence of azimuth compression [see Fig. 7(c)]. The nadir signal is then removed (in this case simply by setting to zero few azimuth lines corresponding to the range, from

[2]In particular, the quadratic variation of the shifts in (3) leads to a tilted linear pattern of the useful signal in the range-compressed data, which allows a uniform distribution of the energy over the range.

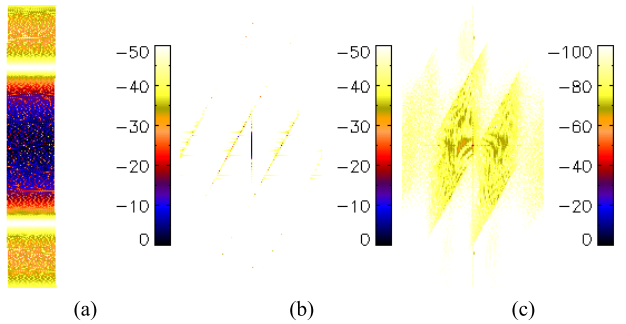

Fig. 6. Simulation for the scenario with two point-like targets, in case the sequence of waveforms of (2) and (3) is employed, but the data are simply focused using a filter "matched" to the useful signal. (a) Raw data with superimposed useful signal and nadir echo. (b) Range-compressed data with useful signal focused at the right location and nadir echo focused at different ranges within the synthetic aperture. (c) Focused data with nadir echo smeared in both range and azimuth. The horizontal and vertical axes represent slant range and azimuth, respectively. All data are displayed in decibels.

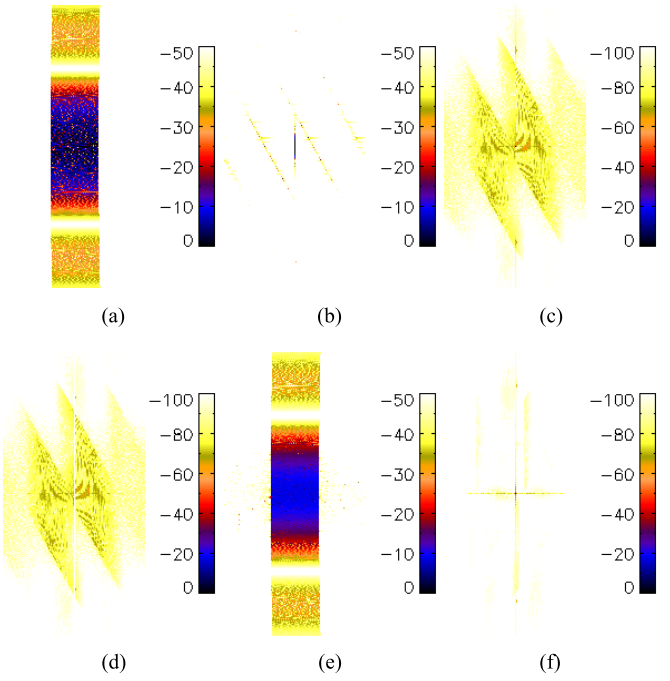

Fig. 7. Simulation for the scenario with two point-like targets, in case the sequence of waveforms of (2) and (3) is employed and data are focused according to the proposed technique. (a) Raw data with superimposed useful signal and nadir echo. (b) Range-compressed data with nadir echo focused at the right location and useful signal focused at different ranges within the synthetic aperture. (c) Focused data with focused nadir echo and useful signal smeared in both range and azimuth. (d) Focused data, in which the nadir echo has been removed by setting to zero three azimuth lines. (e) Raw data obtained by inverse focusing of the data of (d). (f) Focused data, in which the useful signal is focused and the nadir echo has been removed. The horizontal and vertical axes represent slant range and azimuth, respectively. All data are displayed in decibels.

which the nadir echo is expected to come), focused data are then transformed into raw data through an inverse filtering operation, and raw data are finally focused with a filter "matched" to the signal. Setting only three azimuth lines to zero, the nadir echo energy has been attenuated by 22.9 dB, while the signal energy has been attenuated by only 0.0004 dB.

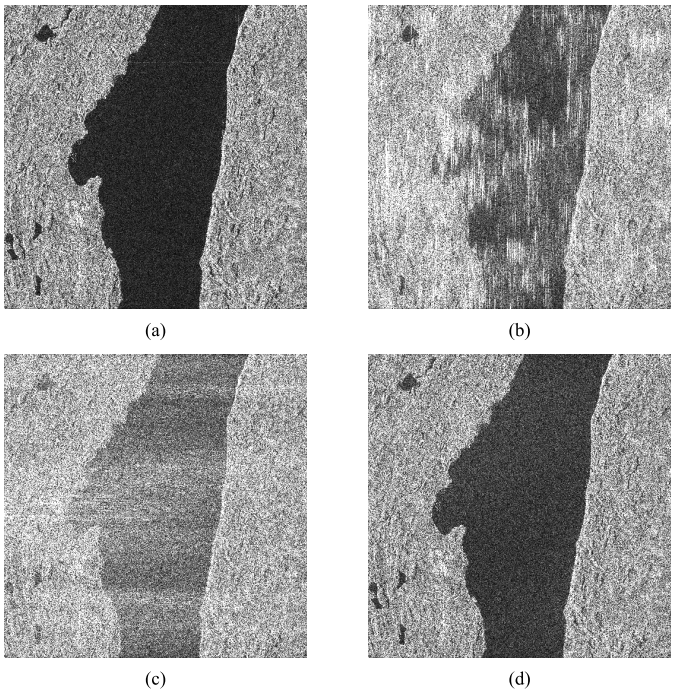

Fig. 8. Impact of mere waveform diversity on image quality using simulated data. (a) Reference, ambiguity-free image. (b) Image corrupted by strong range ambiguities for a conventional SAR without waveform diversity. (c) Image corrupted by the same range ambiguities as (b) for an SAR with up- and down-chirp alternation. Ambiguities are smeared in the range direction. (d) Image corrupted by the same range ambiguities as (b) for an SAR with waveform diversity. Ambiguities appear as a noise-like disturbance rather than localized artifacts and their energy is moreover reduced.

The remaining nadir echo contribution is mainly associated with its first-order azimuth ambiguities, which are slightly displaced in range and could be suppressed by blanking further azimuth lines.

IV. Conclusion

A novel SAR concept has been proposed, which allows designing an SAR system without the nadir interference constraint, i.e., only with the transmit interference constraint, and removing (not only smearing) the nadir echo through waveform diversity on transmit in combination with an appropriate dual-focus postprocessing. This invention yields significant benefits for the design of novel SAR systems, since it increases the design flexibility at the reasonable cost of employing different waveforms on transmit.

This technique can also be used to suppress range ambiguities in SAR images, although the range-ambiguous echoes are not located at specific known ranges, but can be present at different range and azimuth locations. The processing steps are very similar to those for nadir echo suppression (Fig. 3) with the difference that the first three steps (i.e., focusing matched to the range ambiguity, removal of the range-ambiguous signal, and inverse filtering) shall be repeated for all range ambiguities to be suppressed. As far as the suppression of each range-ambiguous signal is concerned, this could be based on an adaptive threshold (based, e.g., on local contrast minimization) to be applied to the image obtained after focusing matched to that range-ambiguous signal.

While further investigations are needed, it is important to state that the mere use of the waveform sequence of (2) and (3) leads to uniform range ambiguity smearing over the pulsewidth and the synthetic aperture (in the case of up- and down-chirp alternation ambiguities are smeared only over the pulselength), as well as some range-ambiguous energy suppression (on the order of 2 dB for the parameters of Table I, while no ambiguity suppression occurs for up- and down-chirp alternation). Similarly to a staggered SAR system, in fact, the ambiguous energy is incoherently integrated in azimuth, spread almost uniformly across the Doppler spectrum, and a part of it is filtered out during SAR processing, if the PRF of the system is larger than its processed Doppler bandwidth [12].

In order to better show the impact of mere waveform diversity on image quality, simulated SAR data have been generated using a TerraSAR-X image acquired over the Greater Munich area, Germany. From the complex backscatter of a part of the image (i.e., the Lake Starnberg), it is possible to generate raw data as they would have been acquired by an SAR system characterized by the parameters of Table I, both without and with waveform diversity, and focus them, obtaining the "ambiguity-free" SAR image in Fig. 8(a). Analogously, the amplitude-scaled complex backscatter of a different part of the image (i.e., the Munich urban area) can be used to simulate range ambiguities, which are then superimposed onto the ambiguity-free SAR image. For a 10-dB amplitude scaling of the ambiguity (this is an extreme case, as a much higher attenuation is expected from the two-way elevation antenna pattern), Fig. 8(b)–(d) shows the resulting corruption of the SAR image due to range ambiguities for a conventional SAR without waveform diversity, an SAR with up- and down-chirp alternation, and an SAR with waveform diversity using the sequence of waveforms of (2) and (3), respectively. For the conventional SAR without waveform diversity, slightly defocused artifacts can be observed over the lake, and for an SAR with up- and down-chirp alternation, ambiguities are smeared only in the range direction. In contrast, for an SAR with waveform diversity using the sequence of waveforms of (2) and (3), ambiguities appear in the image as a noise-like disturbance with reduced energy rather than localized artifacts.

REFERENCES

[1] A. Moreira, P. Prats-Iraola, M. Younis, G. Krieger, I. Hajnsek, and K. P. Papathanassiou, "A tutorial on synthetic aperture radar," *IEEE Geosci. Remote Sens. Mag.*, vol. 1, no. 1, pp. 6–43, Mar. 2013.

[2] J. C. Curlander and R. N. McDonough, *Synthetic Aperture Radar: Systems and Signal Processing*. New York, NY, USA: Wiley, 1991

[3] J. Balkoski and F. Bordoni, "Nadir echo properties, a study based on TerraSAR-X data," in *Proc. TELFOR*, Belgrade, Serbia, Nov. 2012, pp. 420–423.

[4] M. Villano, G. Krieger, and A. Moreira, "Verfahren und Vorrichtung zur rechnergestützten Verarbeitung von SAR Rohdaten," German Patent DE 10 2017 205 649, Dec. 5, 2017.

[5] R. O. Harger, *Synthetic Aperture Radar Systems: Theory and Design*. New York, NY, USA: Academic, 1970.

[6] U. Stein and M. Younis, "Suppression of range ambiguities in synthetic aperture radar systems," in *Proc. EUROCON*, Ljubljana, Slovenia, Sep. 2003, pp. 417–421.

[7] J. Mittermayer and J. M. Martínez, "Analysis of range ambiguity suppression in SAR by up and down chirp modulation for point and distributed targets," in *Proc. IGARSS*, Toulouse, France, Jul. 2003, pp. 4077–4079.

[8] G. Krieger, "MIMO-SAR: Opportunities and pitfalls," *IEEE Trans. Geosci. Remote Sens.*, vol. 52, no. 5, pp. 2628–2645, May 2014.

[9] J. Dall and A. Kusk, "Azimuth phase coding for range ambiguity suppression in SAR," in *Proc. IGARSS*, Anchorage, AK, USA, Sep. 2004, pp. 1734–1737.

[10] G. Krieger, N. Gebert, and A. Moreira, "Multidimensional waveform encoding: A new digital beamforming technique for synthetic aperture radar remote sensing," *IEEE Trans. Geosci. Remote Sens.*, vol. 46, no. 1, pp. 31–46, Jan. 2008.

[11] A. Moreira and T. Misra, "On the use of the ideal filter concept for improving SAR image quality," *J. Electromagn. Waves Appl.*, vol. 9, no. 3, pp. 407–420, 1995.

[12] M. Villano, G. Krieger, M. Jäger, and A. Moreira, "Staggered SAR: Performance analysis and experiments with real data," *IEEE Trans. Geosci. Remote Sens.*, vol. 55, no. 11, pp. 6617–6638, Nov. 2017.